Computational Mechanics
https://doi.org/10.1007/s00466-019-01757-5

ORIGINAL PAPER

Multiphysics computation of thermal tissue damage as a consequence of electric power absorption

B. Emek Abali[1] · **Tarek I. Zohdi**[2]

Received: 11 January 2019 / Accepted: 11 August 2019

Abstract
Electrically induced tissue damage is a coupled phenomenon in multiphysics. Conducting electricity produces heat and this increases the temperature. The soft tissue like skin, organs, brain, or muscles is burnt under successive heating. This damage is modeled by using a damage parameter with a corresponding evolution law above a threshold temperature. Electromagnetism, thermomechanics, and damage modeling creates a set of coupled and nonlinear field equations, by solving them with the aid of the finite element method, we compute a realistic example where the tissue absorbs the electric energy, converts to heat, and gets burnt due to the excessive temperature increase.

Keywords Electromagnetism · Thermodynamics · Damage modeling · Fung's model · Finite element method

1 Introduction

There are countless accidents of burnt tissue as a consequence of conducting electric field over the skin or organs. Depending on the effective current, $\boldsymbol{\jmath}^{\text{fr.}}$, conducting through the tissue because of the electric field, $\boldsymbol{\mathcal{E}}$, an amount of heat is produced that is called JOULE's heat, $\boldsymbol{\jmath}^{\text{fr.}} \cdot \boldsymbol{\mathcal{E}}$. This electrical power is the energy per time generated and mostly absorbed by the tissue because of its inherent exponential response character, which is commonly modeled by the so-called FUNG model. Whenever this power is high, we may consider a case that the whole energy is absorbed by the tissue, in other words, no heat conduction occurs in the system such that the temperature increase is fast and fatal. This excessive energy absorption is often the accident, where the useful electric energy is flowing over the human body instead of the electric circuit as it was designed. Such a fast temperature increase leads to third or fourth degree burning of tissue, resulting in a loss of elasticity (stiffening) and humidity such that a dry and charred material is left over. We call this state "damaged" material. For different levels of burnt tissue as well as their fatality, we refer readers to [13,14,17,31,44].

In this work, we aim at modeling the temperature induced damage in the soft material as a consequence of high current flow through resistive biological tissue. First, we briefly explain the thermodynamics of such a system by using MAXWELL equations and balance equations by following [41] as well as [5]. Second, we obtain the weak form for the computation by following [2]. All computational work has been established by using open-source packages in Python [38] developed under the FEniCS project [8,33]. We emphasize that all field equations are coupled, hence, the strength of the presented approach lies in the monolithic solution method of all unknowns. Third, we create an example where the damage can be visualized clearly. We use FUNG's material model with a phenomenological damage evolution law as in [47] such that the computational analysis herein is expected to be qualitatively representative. We will use the following assumptions in the modeling:

- The material is not polarized.
- Thermal damage is characterized by the stiffening being tantamount to the loss of compliance.
- Plastic deformation fails to occur such that the material is assumed to be hyperelastic or damaged.

✉ B. Emek Abali
bilenemek@abali.org

Tarek I. Zohdi
zohdi@berkeley.edu

[1] Institute of Mechanics, Technische Universität Berlin, Berlin, Germany

[2] Department of Mechanical Engineering, University of California, Berkeley, USA

Published online: 22 August 2019

- No healing can happen in the short time segment of burning the tissue such that the damage is monotonically increasing, its evolution law is zero or positive.

Lightning is a source of very high electric current around 10 kA for a short amount of time, approximately 50 ms. This high energy release is an example for burnt tissue because of JOULE's heat caused elevated temperatures in the body. According to [21], only in the USA up to 300 deaths are estimated annually caused by more than 20 million cloud-to-ground lightning strikes. We demonstrate the robustness of the underlying algorithm by performing a simplified simulation of damage realized in extremities caused by a lightning.

2 Governing equations

Thermodynamics sets the objective to calculate mass density, ρ, velocity, $\boldsymbol{v}$, temperature, T, electric field, $\boldsymbol{\mathcal{E}}$, and magnetic flux (area density), $\boldsymbol{B}$, as functions in space and time. All these quantities are determined in a so-called laboratory frame. For solid body mechanics, it is beneficial to understand the current placement of particles as the particles occupying the spatial position $\boldsymbol{x}$ in the laboratory frame. Hence, by tracking particles' positions, we create a material system with a reference frame usually chosen as the initial frame since we know the spatial positions of continuum body's particles at the initial time, $t = 0$. We consider a continuum body, occupying $\mathcal{B}_0$ initially, with a given mass density ρ_0 in this initial frame. The space coordinates, $\boldsymbol{X}$, denote material particles; we introduce the motion to the current position, $\boldsymbol{x} = \boldsymbol{u} + \boldsymbol{X}$ with the displacement, $\boldsymbol{u}$, by using the deformation gradient and its determinant,

$$F_{ij} = \frac{\partial x_i}{\partial X_j} = \frac{\partial u_i}{\partial X_j} + \delta_{ij} = u_{i,j} + \delta_{ij} \ , \quad J = \det(\boldsymbol{F}), \tag{1}$$

expressed by Cartesian coordinates; where all Latin indices run one to three in three-dimensional continuum, $\mathcal{B}_0 \in \mathbb{R}^3$. We use the conventional continuum mechanics notation with EINSTEIN's summation convention applied to every repeated indices and a comma notation indicating that a partial space derivative is taken. The KRONECKER delta, $\boldsymbol{\delta}$, is the identity matrix and the deformation gradient is used to transform or map the balance equations of mass, momentum, and energy from the current to the initial frame. In the case of electromagnetism, the transformation is challenging, we refer to [28] and [4]. In this work, we assume small deformations with respect to the geometric dimensions such that the transformation from the current to the initial frame is circumvented. Technically, we use MAXWELL equations in the current frame and the balance equations in the initial frame. Effected by the assumption of small deformations, we skip a distinction between them. This assumption is admissible for the application even in the case we use a material model being capable of representing large deformations.

After a straightforward derivation as in [3] as well as in [2, Sect. 2.4 and 3.3], we obtain the balance of internal energy in the initial frame

$$\rho_0 \dot{u} + Q_{i,i} - \rho_0 r = J \mathcal{J}_i \mathcal{E}_i + S_{ij} \dot{\mathcal{E}}_{ij}, \tag{2}$$

with the specific internal energy u, heat flux $\boldsymbol{Q}$, 2nd PIOLA–KIRCHHOFF stress $\boldsymbol{S}$, and GREEN–LAGRANGE strain $\boldsymbol{\mathcal{E}} = (\boldsymbol{C} - \boldsymbol{\delta})/2$ with the right CAUCHY–GREEN deformation tensor, $\boldsymbol{C} = \boldsymbol{F}^{\mathsf{T}} \boldsymbol{F}$. We write on the right-hand side the production term as usual in the non-equilibrium thermodynamics. We emphasize that no polarization is assumed such that $\boldsymbol{\mathcal{J}}^{\text{fr.}} = \boldsymbol{\mathcal{J}}$ in this work. The first production term in Eq. (2) is the JOULE heating causing the temperature increase in the application. The stress can be decomposed into reversible and irreversible terms, in this work, we assume that the irreversible stress—caused by the viscous character of the material—is not significant. In other words, we assume that the tissue behaves elastic until the damage. By introducing the HELMHOLTZ free energy per mass,

$$f = u - T\eta, \tag{3}$$

with the specific entropy η, we reformulate Eq. (2) and obtain the balance of entropy,

$$\begin{aligned} &\rho_0 \dot{f} + \rho_0 \dot{T} \eta + \rho_0 T \dot{\eta} + Q_{i,i} - \rho_0 r = J \mathcal{J}_i \mathcal{E}_i + S_{ij} \dot{\mathcal{E}}_{ij}, \\ &\rho_0 \dot{\eta} + \left(\frac{Q_i}{T}\right)_{,i} - \rho_0 \frac{r}{T} = -\frac{Q_i}{T^2} T_{,i} \\ &\quad + \frac{J}{T} \mathcal{J}_i \mathcal{E}_i + \frac{1}{T}\left(S_{ij} \dot{\mathcal{E}}_{ij} - \rho_0 \dot{f} - \rho_0 \dot{T} \eta\right) \end{aligned} \tag{4}$$

where the right hand side is the entropy production, Σ, which has to satisfy $\Sigma \geq 0$ according to the 2nd law of thermodynamics. By assuming that the internal energy is reversible, we acquire $f = f(T, \boldsymbol{\mathcal{E}})$ with the following identities leading to a vanishing final term in the entropy production,

$$\eta = -\frac{\partial f}{\partial T} \ , \qquad S_{ij} = \rho_0 \frac{\partial f}{\partial \mathcal{E}_{ij}}. \tag{5}$$

Then the usual choice of the heat flux as well as the electric current,

$$Q_i = -\kappa T_{,i} + \varsigma \pi T \mathcal{E}_i \ , \qquad \mathcal{J}_i = \varsigma \pi T_{,i} + \varsigma \mathcal{E}_i, \tag{6}$$

gives the only admissible constitutive relations with $\kappa \geq 0$ and $\varsigma \geq 0$ such that the entropy production is zero or positive, $\Sigma \geq 0$. The thermoelectric constant π is often neglected. In this case, if the thermal conductivity, κ, is constant, the constitutive relation for $\boldsymbol{Q}$ is named after FOURIER; analogously,

if the electric conductivity, ς, is constant, the relation for $\boldsymbol{\jmath}$ is called OHM's law. The choice of the free energy is established in a phenomenological manner. Especially for soft materials, its description is discussed heavily in the literature, among others we refer to [27] as well as [26]. By following [2, Sect. 2.4], in the case of no damage, and also neglecting the thermal expansion, the relatively simple energy and entropy read

$$u = c(T - T_{\text{ref.}}) + \frac{1}{2\rho_0}\mathcal{E}_{ij}C_{ijkl}\mathcal{E}_{kl}\,, \qquad \eta = c\ln\Big(\frac{T}{T_{\text{ref.}}}\Big), \tag{7}$$

where the specific heat capacity, c, is assumed to be a constant material parameter. The reference temperature will be set to the room temperature, $T_{\text{ref.}} = 300\,\text{K}$, and the stiffness tensor, C_{ijkl}, is the inverse of the compliance—compliance is a measurable material parameter, we refer to [9, Sect. 2.1.4] for a clear explanation of such measurements. By using Eqs. (3), $(5)_2$, we obtain the 2nd PIOLA–KIRCHHOFF stress from the energy,

$$S_{ij} = \rho_0\frac{\partial f}{\partial \mathcal{E}_{ij}} = C_{ijkl}\mathcal{E}_{kl}. \tag{8}$$

In order to acquire a formulation for tissue type soft materials, we follow [19,20], as throughly discussed in [47], and introduce the following internal energy, called the FUNG material model:

$$u = c(T - T_{\text{ref.}}) + \frac{1}{2\rho_0}\mathcal{E}_{ij}H_{ijkl}\mathcal{E}_{kl} + \frac{D}{\rho_0}\Big(\exp\Big(\frac{1}{2}\mathcal{E}_{ij}B_{ijkl}\mathcal{E}_{kl}\Big) - 1\Big), \tag{9}$$

where H_{ijkl}, D, and B_{ijkl} are material parameters. We acquire the stress,

$$S_{ij} = \rho_0\frac{\partial f}{\partial \mathcal{E}_{ij}} = H_{ijkl}\mathcal{E}_{kl} + DB_{ijkl}\mathcal{E}_{kl}\exp\Big(\frac{1}{2}\mathcal{E}_{mn}B_{mnop}\mathcal{E}_{op}\Big), \tag{10}$$

which has to match the stress in Eq. (8) as strain converges to zero. This condition leads to the following assertion:

$$H_{ijkl} + DB_{ijkl} = C_{ijkl}. \tag{11}$$

Now, we employ a simplification and choose $H_{ijkl} = 0$ such that the material parameter for the FUNG model is determined by knowing the stiffness tensor and estimating D in the simulation,

$$B_{ijkl} = \frac{1}{D}C_{ijkl}. \tag{12}$$

Furthermore, by following [29], one possible approach to implement the damage relies on using a simple model with a scalar damage variable, α, as follows:

$$C_{ijkl} = \frac{1}{\alpha}C^0_{ijkl}. \tag{13}$$

Therefore, in the case of damage, the internal energy reads

$$u = c(T - T_{\text{ref.}}) + \frac{D}{\rho_0}\Big(\exp\Big(\frac{1}{2D\alpha}\mathcal{E}_{ij}C^0_{ijkl}\mathcal{E}_{kl}\Big) - 1\Big), \tag{14}$$

such that the free energy depends on the damage variable as well, $f = f(T, \mathcal{E}, \alpha)$. The dependencies on the temperature and the strain generated Eq. (5), now by adding the dependency on the damage variable, by inserting $f = f(T, \mathcal{E}, \alpha)$ into Eq. (4), we obtain the following entropy production:

$$\begin{aligned}\Sigma &= -\frac{Q_i}{T^2}T_{,i} + \frac{J}{T}\mathcal{J}_i\mathcal{E}_i \\ &\quad + \frac{1}{T}\Big(S_{ij}\dot{\mathcal{E}}_{ij} - \rho_0\Big(\frac{\partial f}{\partial T}\dot{T} + \frac{\partial f}{\partial \mathcal{E}_{ij}}\dot{\mathcal{E}}_{ij} + \frac{\partial f}{\partial \alpha}\dot{\alpha}\Big) - \rho_0\dot{T}\eta\Big)\,, \\ \Sigma &= -\frac{Q_i}{T^2}T_{,i} + \frac{J}{T}\mathcal{J}_i\mathcal{E}_i - \frac{\rho_0}{T}\frac{\partial f}{\partial \alpha}\dot{\alpha}.\end{aligned} \tag{15}$$

According to the so-called CURIE principle, the same type of tensors depend on each other. We conclude that $\partial f/\partial\alpha$ and $\dot{\alpha}$ may be related to each other in such a way that the product is positive

$$-\frac{\rho_0}{T}\frac{\partial f}{\partial \alpha}\dot{\alpha} \geq 0. \tag{16}$$

This relation is an assertion of the 2nd law of thermodynamics and arises naturally, it is often seen as an additional condition and called the KARUSH–KUHN–TUCKER relation originally used in plasticity, see [40]. By taking the derivative, we observe

$$\frac{\mathcal{E}_{ij}C^0_{ijkl}\mathcal{E}_{kl}}{2T\alpha^2}\exp\Big(\frac{1}{2D\alpha}\mathcal{E}_{mn}C^0_{mnop}\mathcal{E}_{op}\Big)\dot{\alpha} \geq 0, \tag{17}$$

such that rate of the damage, $\dot{\alpha}$, has to be positive. This relation is modeled by a phenomenological evolution equation, for example a simple approach reads

$$\dot{\alpha} = \begin{cases} k\dfrac{T - T_{\text{Tr}}}{T_{\text{Tr}}}, & T > T_{\text{Tr}} \\ 0, & T \leq T_{\text{Tr}} \end{cases} \tag{18}$$

where the threshold temperature T_{Tr} controls the start of damage. The damage variable is $1 < \alpha < \infty$ and it increases monotonically with a positive constant, $k \geq 0$. Often, a related parameter $\omega = 1/\alpha$ is used as $0 < \omega < 1$, where

$\omega = 1$ indicates no damage and $\omega = 0$ asserts failure. Of course, the identification of a threshold temperature is very challenging as discussed in [25,35,43]. The proposed simple model in Eq. (18) uses a linear relation between the temperature difference and damage rate. There are ample studies for a more sophisticated damage model as in [25,35] based on the assumption that tissue burning is a chemical process to be modeled by using an ARRHENIUS model, we refer to [45]. Measuring the material parameters in such a model is another difficulty, as discussed in [39]; but there are models providing realistic results, for example, we can use the following ARRHENIUS type of phenomenological evolution equation:

$$\dot{\alpha} = A \exp\Big(-\frac{E_a}{RT}\Big)\,, \quad A = \exp\Big(\frac{E_a - a}{b}\Big), \tag{19}$$

with an activation energy, $E_a = 5 \times 10^5\,\mathrm{J/mol}$, the universal gas constant, $R = 8.314\,\mathrm{J/(mol\,K)}$, and the fit parameters, $a = 21149.324\,\mathrm{J/mol}$ and $b = 2688.367\,\mathrm{J/mol}$ obtained from [46]. However, these fit parameters result in A in the order of 10^{77} making this evolution equation unfeasible for a simulation. Herein we present a general framework for a computation of thermal damage and as an example utilize Eq. (18) in order to demonstrate the usefulness of the suggested framework. Even more sophisticated methods are possible for including healing [16] and porosity [23] or based on the mechanical stress [11].

In order to calculate the displacement, we use the balance of (linear) momentum,

$$\rho_0 \ddot{u}_i - P_{ji,j} - \rho_0 f_i = \mathcal{F}_i, \tag{20}$$

with the PIOLA stress, $P_{ji} = F_{ik} S_{jk}$, given by the stress in Eq. (10); with the known gravitational (specific) force, $\boldsymbol{f}$; and the electromagnetic force density, $\boldsymbol{\mathcal{F}}$. Since the material is non-polarized, the electromagnetic force density is defined by the LORENTZ force density,

$$\mathcal{F}_i = \rho z \mathcal{E}_i + \epsilon_{ijk} \mathcal{J}_j B_k, \tag{21}$$

with the specific (electric) charge, z. We emphasize $\rho = \rho_0$ as a consequence of the assumption of small deformations. The LEVI-CIVITA symbol, ϵ_{ijk}, is the permutation symbol in Cartesian coordinates. For $\boldsymbol{\mathcal{J}}$ we employ the constitutive equation $(6)_2$ and the electric charge will be discussed in the following.

In order to calculate the electromagnetic fields, $\boldsymbol{E}$, $\boldsymbol{B}$, we follow the procedure as in [2, Sect. 3.2]. First, we introduce FARADAY's law and derive the following MAXWELL equations,

$$B_{i,i} = 0\,, \quad \frac{\partial B_i}{\partial t} + \epsilon_{ijk} E_{k,j} = 0, \tag{22}$$

with the usual transformation between the electric field in the laboratory frame, E_i, and the electric field in the material frame, $\mathcal{E}_i$, as follows:

$$E_i = \mathcal{E}_i - \epsilon_{ijk} \dot{u}_j B_k. \tag{23}$$

A solution of Eq. (22) is obtained by the ansatz functions:

$$E_i = -\phi_{,i} - \frac{\partial A_i}{\partial t}\,, \quad B_i = \epsilon_{ijk} A_{k,j}, \tag{24}$$

where the electromagnetic potentials ϕ, $\boldsymbol{A}$ need to be calculated. This solution is not unique since we fail to determine six functions of $\boldsymbol{E}$, $\boldsymbol{B}$ uniquely by using four functions of ϕ, $\boldsymbol{A}$. The missing two values of $A_{i,i}$ and $\partial\phi/\partial t$ have to be set. They can be chosen arbitrarily, which is often called the gauge freedom. We will use LORENZ's gauge [34]. Second, we introduce the balance of electric charge and derive the following MAXWELL equations,

$$D_{i,i} = \rho z\,, \quad -\frac{\partial D_i}{\partial t} + \epsilon_{ijk} H_{k,j} = J_i, \tag{25}$$

where the charge potential, $\boldsymbol{D}$, and the current potential, $\boldsymbol{H}$, are given by the MAXWELL–LORENTZ aether relations:

$$D_i = \varepsilon_0 E_i\,, \quad H_i = \frac{1}{\mu_0} B_i, \tag{26}$$

with the universal constants:

$$\begin{aligned} \varepsilon_0 &= 8.85 \cdot 10^{-12}\,\mathrm{A\,s/(V\,m)}\,, \\ \mu_0 &= 12.6 \cdot 10^{-7}\,\mathrm{V\,s/(A\,m)}. \end{aligned} \tag{27}$$

The electric current in the laboratory frame, $\boldsymbol{J}$, is given by,

$$J_i = \mathcal{J}_i + \rho z \dot{u}_i. \tag{28}$$

For solving the electric potential, ϕ, we use the balance of electric charge,

$$\frac{\partial \rho z}{\partial t} + J_{i,i} = 0, \tag{29}$$

augmented by Eq. $(25)_1$. In order to solve the magnetic potential, $\boldsymbol{A}$, we use the MAXWELL equation $(25)_2$, augmented by the LORENZ gauge:

$$\frac{\partial \phi}{\partial t} + \frac{1}{\varepsilon_0 \mu_0} A_{i,i} = 0. \tag{30}$$

For summing up, we aim at solving temperature, T, displacement, $\boldsymbol{u}$, electric field, $\boldsymbol{\mathcal{E}}$, and magnetic flux, $\boldsymbol{B}$, by satisfying the governing equations $(4)_2$, (20), (25), (29) with aforementioned constitutive equations with the damage parameter

defined by a phenomenological evolution equation (18). This coupled and nonlinear system can be solved numerically. We will use a variational formulation for generating the weak form and employ the finite difference method in time as well as the finite element method in space for solving the system monolithically.

3 Variational formulation

We set the objective as computing $\{\phi, \boldsymbol{A}, \boldsymbol{u}, T\}$ as continuous functions in space and time. Although we use the material frame, by using the small deformation assumption, we circumvent a discussion about the correct transformation of MAXWELL equations onto the material frame. By using the aforementioned governing equations, we suggest a simple approach leading to the weak form as follows:

1. Discretize in time,
2. Multiply by an arbitrary test function,
3. Discretize in space and integrate over the computational domain,
4. Integrate by parts the necessary terms,
5. Apply jump conditions.

Each of these are explained in detail in previous works, see [2,5] for electro-magneto-thermo-mechanical applications. We emphasize that a fully monolithic solution approach is developed increasing the accuracy of coupling terms [6] as well as strengthening the robustness of the algorithm. We undertake the steps and obtain the weak form. By using finite difference method in the time discretization, we obtain an approach that is often called EULER backwards method and it is unconditionally stable (for problems with real numbers). In the material frame, rate of every quantity equals to the partial time derivative that is discretized at the current time, t, as follows:

$$()^{\cdot} = \frac{\partial ()}{\partial t} = \frac{() - ()^0}{\Delta t}, \tag{31}$$

where the superscript ^{0} denotes the known value at the last time step, $t - \Delta t$. We use the same time step, Δt, throughout the simulation.

For computing $\{\phi, \boldsymbol{A}, \boldsymbol{u}, T\}$ we use the test functions $\{\delta\phi, \delta\boldsymbol{A}, \delta\boldsymbol{u}, \delta T\}$ from the same HILBERTian SOBOLEV space, we refer to [49] for details of the finite element method. Basically, we use

$$\mathcal{V} = \left\{ \{\phi, \boldsymbol{A}, \boldsymbol{u}, T\} \in [\mathcal{H}^1(\Omega)]^8 : \{\phi, \boldsymbol{A}, \boldsymbol{u}, T\}\Big|_{\partial\Omega} = \text{given} \right\}, \tag{32}$$

within the computational domain, Ω, by utilizing the "standard" continuous GALERKIN elements with linear shape functions for all fields. We stress that this choice is unusual for the case of electromagnetism. Often, this approach fails to converge such that special elements are used [36,42] or different strategies are developed as in [10,12,22,32,37] and [15, Sect. 17]. By using standard elements instead of mixed elements, we can assure a monotonous convergence even in this coupled system and compute realistic applications as demonstrated in [7,48]. Hence, using standard elements is beneficial and possible by following the presented approach herein. Two important factors help this approach to work, one is the applied LORENZ gauge and another one is implementation of the jump conditions in electromagnetism.

For the sake of a simplified notation, we skip a distinction between the analytic functions and their numerical approximations since they never occur in the same formulation. For the weak form of electric potential, ϕ, we use Eq. (28) and obtain

$$\mathrm{F}_\phi = \int_\Omega \left(-(D_i - D_i^0)\delta\phi_{,i} - \Delta t\, J_i \delta\phi_{,i} \right) \mathrm{d}V + \int_\Gamma n_i \Delta t [\![J_i]\!] \delta\phi \, \mathrm{d}A, \tag{33}$$

in the unit of energy. On the interface, Γ, between two different materials, say $+$ and $-$, the jump of the electric current, $[\![\boldsymbol{J}]\!] = \boldsymbol{J}^+ - \boldsymbol{J}^-$, is caused by the difference of the electric conductivity of materials. On the domain's boundary, $\partial\Omega$, we set the value of the electric potential as a DIRICHLET boundary condition. As a specific case, herein, we assume that the continuum body has no jump terms on the boundary being tantamount to isolated boundaries as if the body is embedded in air. Hence, the final term drops and we solve

$$\mathrm{F}_\phi = \int_\Omega \left(-(D_i - D_i^0)\delta\phi_{,i} - \Delta t\, J_i \delta\phi_{,i} \right) \mathrm{d}V. \tag{34}$$

Analogously, for the weak form of the magnetic potential, $\boldsymbol{A}$, we obtain first from Eq. (25) with Eq. (30) the following governing equation:

$$\varepsilon_0 \frac{\partial^2 A_i}{\partial t^2} - \frac{1}{\mu_0} A_{i,jj} = J_i \ , \qquad A_{i,jj} = \frac{\partial^2 A_i}{\partial X_j \partial X_j}. \tag{35}$$

Its weak form is established by multiplying by the test function, $\delta\boldsymbol{A}$, integrating by parts, applying the jump conditions and neglecting polarization, as follows:

$$\mathrm{F}_{\boldsymbol{A}} = \int_\Omega \left(\varepsilon_0 \frac{A_i - 2A_i^0 + A_i^{00}}{\Delta t \Delta t} \delta A_i + \frac{1}{\mu_0} A_{i,j} \delta A_{i,j} - J_i \delta A_i \right) \mathrm{d}V, \tag{36}$$

in the unit of energy. For electromagnetic potentials, we need to solve a bigger domain than necessary in order to set the far-away boundaries zero. Herein, the application is not about the fields around the body and we assume that neglecting them fails to introduce any significant error. In order to compute the displacement, we use the balance of linear momentum as in Eq. (20) and obtain the weak form in the unit of energy,

$$\mathrm{F}_{\boldsymbol{u}} = \int_\Omega \left(\rho_0 \frac{u_i - 2u_i^0 + u_i^{00}}{\Delta t \Delta t} \delta u_i + P_{ji} \delta u_{i,j} - \rho_0 f_i \delta u_i - \mathcal{F}_i \delta u_i \right) \mathrm{d}V. \tag{37}$$

The boundaries vanish for the clamped end by using DIRICHLET conditions and also for the other boundaries by assuming free boundaries. For computing temperature we employ the balance of entropy in Eqs. $(4)_2$ and obtain the weak form in the unit of energy,

$$\mathrm{F}_T = \int_\Omega \left(\rho_0 (\eta - \eta^0) \delta T - \Delta t \frac{Q_i}{T} \delta T_{,i} - \Delta t \rho_0 \frac{r}{T} \delta T - \Delta t \Sigma \delta T \right) \mathrm{d}V + \int_{\partial\Omega} \frac{\Delta t}{T} h (T - T_{\text{ref.}}) \delta T \, \mathrm{d}A, \tag{38}$$

with the entropy production:

$$\Sigma = -\frac{Q_i}{T^2} T_{,i} + \frac{J}{T} \mathcal{J}_i \mathcal{E}_i + \frac{\mathcal{E}_{ij} C^0_{ijkl} \mathcal{E}_{kl}}{2T\alpha^2} \exp\left(\frac{1}{2D\alpha} \mathcal{E}_{mn} C^0_{mnop} \mathcal{E}_{op} \right) \dot{\alpha}, \tag{39}$$

where for boundaries, we readily applied the natural boundary condition, $Q_i N_i = h(T - T_{\text{ref.}})$, with an ambient temperature chosen as the reference (initial) temperature. The nonlinear weak form is the sum of Eqs. (34), (36)–(38), i.e.,

$$\text{Form} = \mathrm{F}_\phi + \mathrm{F}_{\boldsymbol{A}} + \mathrm{F}_{\boldsymbol{u}} + \mathrm{F}_T, \tag{40}$$

with the following constitutive equations:

$$\begin{aligned} D_i &= \varepsilon_0 E_i \,, \quad H_i = \frac{1}{\mu_0} B_i \,, \\ S_{ij} &= C_{ijkl} \mathcal{E}_{kl} \exp\left(\frac{1}{2D} \mathcal{E}_{ij} C_{ijkl} \mathcal{E}_{kl} \right) \\ \eta &= c \ln\left(\frac{T}{T_{\text{ref.}}} \right) , \\ Q_i &= -\kappa T_{,i} + \varsigma \pi T \mathcal{E}_i \,, \quad \mathcal{J}_i = \varsigma \pi T_{,i} + \varsigma \mathcal{E}_i \,, \end{aligned} \tag{41}$$

where $C_{ijkl} = \omega C^0_{ijkl}$ and $\omega = 1/\alpha$ with an update of the damage parameter in each time step,

$$\alpha := \alpha + \Delta t \dot{\alpha}, \tag{42}$$

where the evolution is given by

$$\dot{\alpha} = \begin{cases} k \dfrac{T - T_{\text{Tr}}}{T_{\text{Tr}}}, & T > T_{\text{Tr}} \\ 0, & T \le T_{\text{Tr}} \end{cases} \tag{43}$$

The material parameters, C_{ijkl}, D, κ, π, c, and ς are constant. For an isotropic material,

$$C_{ijkl} = \lambda \delta_{ij} \delta_{kl} + \mu \delta_{ik} \delta_{jl} + \mu \delta_{il} \delta_{jk}, \tag{44}$$

is given by LAME parameters, λ, μ, in connection with the so-called engineering constants, YOUNG's modulus, E, and POISSON's ratio, ν, as follows:

$$\lambda = \frac{E\nu}{(1+\nu)(1-2\nu)} \,, \quad \mu = \frac{E}{2(1+\nu)}. \tag{45}$$

4 Computational example

For solving the set of coupled and nonlinear partial differential equations represented by the weak form in Eq. (40), we employ the open source packages developed under the FEniCS project by using the parameters collected from [18, Table 8.12] and [46], compiled in Table 1. We emphasize that the solution of all unknowns are obtained at once. Therefore, in each node, 8 unknowns, $\{\phi, A_1, A_2, A_3, u_1, u_2, u_3, T\}$ are computed in three-dimensional space leading to a large system to solve. All computation has been established by the open-source codes called FEniCS. Standard NEWTON–RAPHSON linearization is used by linearizing the system at the partial differential equations' level with symbolic differentiation. Hence, the nonlinear material modeling as well as the nonlinearities introduced in the entropy production have been utilized masterfully without causing any numerical problems. For solving the linearized system, we use the generalized minimal residual method *gmres* as an iterative solver with an algebraic multigrid *amg* preconditioner and an over-relaxation of 1.05 by using parallel computing via *mpirun* on a Ubuntu operating system in one node. We stress that the over-relaxation in an iterative solution is of importance for such a coupled problem with different types of differential equations. The scalability of the algorithm is very high, we have used "only" 20 cores[1] for the problem with 134,904 degrees of freedom for in total 1000 time steps lasting 17 h of computing time. The shown application is one example and by simply changing the geometry and boundary conditions, various examples can be simulated. For motivating the

[1] Intel Xeon Broadwell-EX series E7-4850.

Table 1 Coefficients and material parameters used in the simulation with the following units: mm for length, tonne or mg for mass, s for time, mA for current, K for temperature leading to N, MPa, mJ, mW, V, and μT

Parameter	Variable	Value	Unit
Reference temperature	$T_{\text{ref.}}$	310	K
YOUNG's modulus	E	100	MPa $\hat{=}10^6$ N/m^2
POISSON's ratio	ν	0.45	
Electric conductivity	ς	0.23	mS/mm $\hat{=}$ 1/(Ω m)
Mass density	ρ	1000×10^{-12}	mg/mm^3 $\hat{=}$1000 kg/m^3
Thermal conductivity	κ	0.96	mW/(mm K) $\hat{=}$ W/(m K)
Specific heat capacity	c	3770×10^6	mJ/(mg K) $\hat{=}$3770 J/(kg K)
Convective heat transfer	h	0	mW/(mm^2 K) $\hat{=}10^3$ W/(m^2 K)
PELTIER constant	π	0	V/K
Damage parameter	D	1	
Damage rate	k	0.8	
Threshold temperature	T_{Tr}	330	K

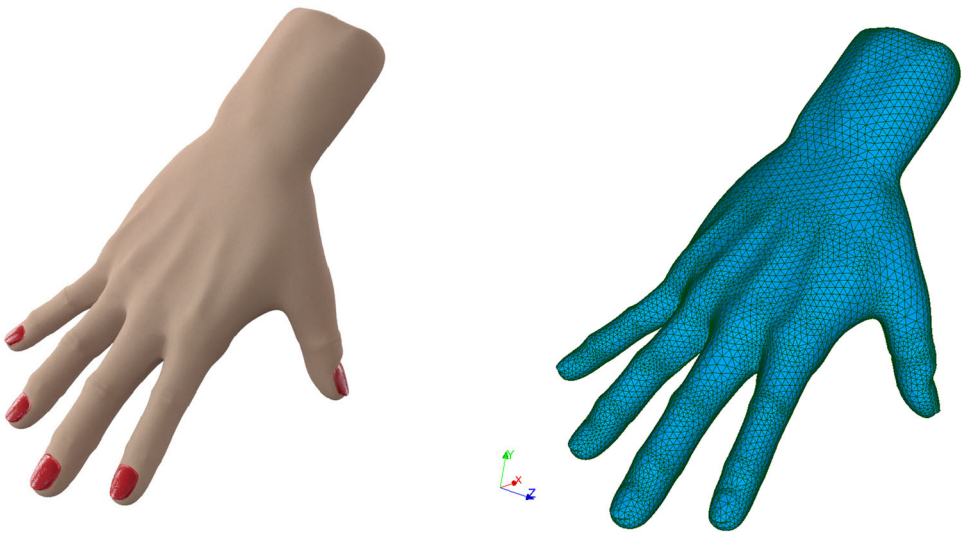

Fig. 1 CAD model of a hand taken from [30]. Left: rendering in SolidWorks [30]. Right: model with tetrahedron mesh of 16,803 nodes generated from the CAD file by using NetGen algorithms in Salome

scientific exchange, we make the code publicly available in [1] to be used under the GNU Public license as in [24].

The application shown here is an electrocution at the extremities caused by a lightning. Consider the following boundary condition:

$$\phi = \phi_{\text{amp}} \sin(2\pi\nu t), \tag{46}$$

where the simulation time is half of the period, $1/(2\nu)$, chosen as 50 ms, which is realistic for a lightning. The amplitude is chosen great enough to obtain a couple of ampere electric current, whereas in a lightning up to 30 kA is possible. A part of the human body, herein the hand as in Fig. 1, is used as ground such that electric current flows over the hand. We simply use the aforementioned boundary condition on one end, namely at the tip of the middle finger, and ground the system by setting the electric potential to zero on the other hand. Indeed in reality, the grounding would be via the feet to the Earth; but the results would be the same since the generated potential difference between the wrist and tip of the finger is decisive. In order to demonstrate the convergence behavior in this coupled and nonlinear problem with the proposed monolithic solution technique, we simply generate three meshes by varying the minimum and maximum sizes of elements in the triangulation as 1, 1.5, and 2. This change leads to almost a 1, 1.5, and 2 times degrees of freedom in the three subsequent meshes. With the aforementioned boundary conditions, at the instant 10 ms, we compile the results of computed quantities, $\boldsymbol{u}, \phi, \boldsymbol{A}, T$, evaluated at the middle of the hand in Table 2. The expected monotonic convergence behavior demonstrates the reliability of the results. Herein we choose the third mesh for further analysis. The (linear) distribution of the electric potential generates an electric current localized at the finger tip as demonstrated in Fig. 2. The displacement fails to be significant as it is solely induced by the electromagnetic fields since we have ignored the thermal expansion.

For simplicity, we model the whole continuum body out of the same material. Technically, especially for the wrist sec-

Table 2 Convergence analysis of the employed algorithm

Degrees of freedom	$\|\boldsymbol{u}\|$ in mm	ϕ in V	$\|\boldsymbol{A}\|$ in μTmm	T in K
68,592	1.686×10^{-4}	40.701×10^{3}	5.699×10^{-7}	527.7
111,008	1.710×10^{-4}	40.554×10^{3}	6.696×10^{-7}	523.6
134,904	1.744×10^{-4}	40.544×10^{3}	6.694×10^{-7}	521.5

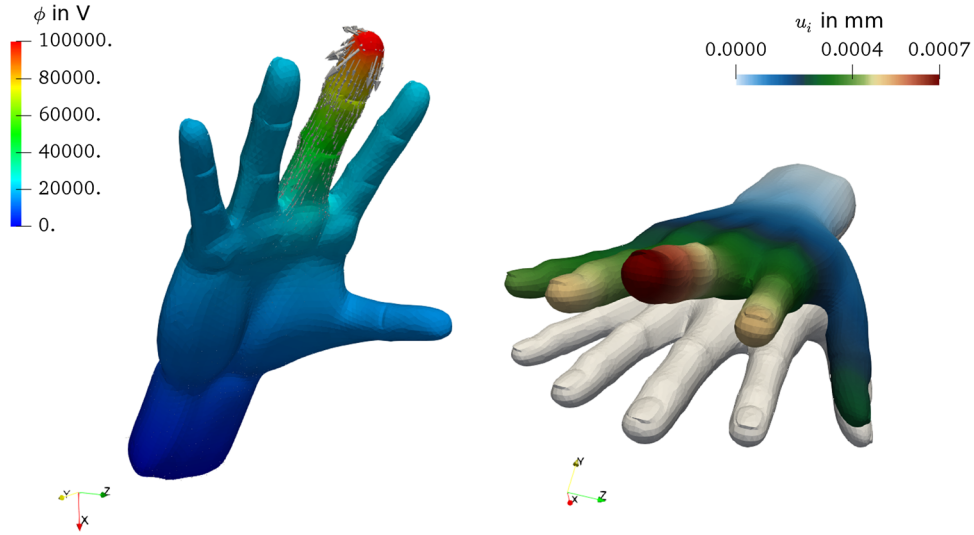

Fig. 2 Simulation results of the electrocution at the maximum of the harmonic electric potential, $t = 25$ ms by using ParaView. Left: the distribution of the electric potential, ϕ, in colors and the electric current, $\boldsymbol{J}$, as scaled arrows. Right: the displacement is shown by scaling the model 50k times for the purpose of visualization. (Color figure online)

tion, we need to model bones and tissue differently. However, modeling with different layers of skin, tissue, and bone sections are simple to construct when the geometry details are present and material parameters are available. Herein, we accomplish a general simulation code and demonstrate its ability to perform such a computation presenting the accumulated damage as a result of JOULE's heat as shown in Fig. 3. We emphasize that the evolution equation is constructed in such a way that the damage parameter only increases (no healing occurs). Indeed, for the simulation lasting only 50 ms, this simplification is easily justified. The distribution of the damage parameter is identical to the temperature, which is steering the evolution of α. For a very short amount of time, the temperature is very high, however, the real measure of the damage is the intensity of the heat over time that be given by an appropriate evolution equation. We have implemented a very simple linear relation and discussed another more sophisticated evolution equation, which is not feasible because of the fit parameters. The code allows to do simulations with that model as well. After a parameter fitting for any evolution equation, depending on the value of the damage parameter, it might be possible to evaluate the seriousness of the accident.

All results are obtained by solving the transient equations at once in each time step, we call this method monolithic in time and emphasize that the accuracy of the coupling between electromagnetism and thermomechanics is the highest possible. By having acquired reliable solutions, we can investigate the roles of each term in the solution for this application. For

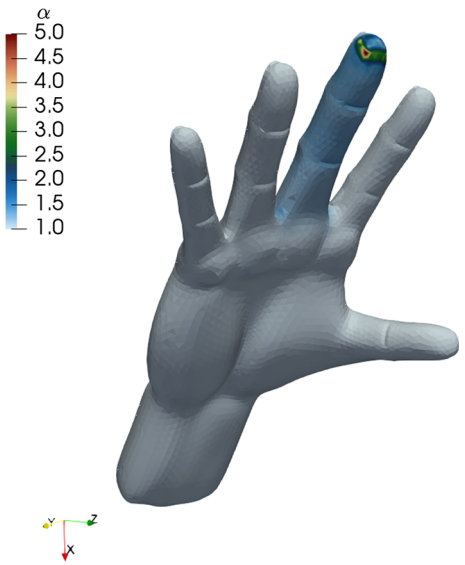

Fig. 3 Simulation results at $t = 50$ ms, the accumulated damage α is shown in color, qualitatively we expect that the maximum damage indicates a burnt tissue. (Color figure online)

example, the deformation is clearly not significant throughout the simulation. As the duration of the application is short and we have left out the thermal expansion, we only simulate the deformation caused by the LORENTZ force. Moreover, the magnetic potential has no significant effect as we are not interested in mechanics affected by the magnetic flux. A counter-example would be the effect of electromagnetism on

blood flow, whereas the blood is magnetized and responds to the electromagnetic fields greatly. The application herein is a demonstration how to extend the general formulation of electromagnetism and thermomechanics for a tissue type material including damage. All governing equations are solved transient in time for alternating current (AC) by using continuous LAGRANGE an finite elements without any simplifications such that the method can be used for other applications as well; the code is to be found in [1] for further use under the GNU Public license as in [24].

5 Conclusion

A general framework has been presented for a tissue type soft matter by using FUNG material model. This formulation includes governing equations for solving electromagnetic and thermomechanical fields all together by means of open-source packages known under FEniCS. The governing equations are nonlinear and coupled; solving them is often restricted by numerical problems, especially in electromagnetism. By using a novel approach, we have obtained governing equations and presented a realistic application, in which the solution of all fields has been realized without any numerical problems by using parallel computing and iterative solvers (with preconditioning). The transient solution of the application under AC has resulted in intuitively correct results for a serious damage resulted by lightning to extremities.

Acknowledgements B. E. Abali's work was partly supported by a Grant from the Daimler and Benz Foundation.

References

1. Abali BE (2016) Technical University of Berlin, Institute of Mechanics, Chair of Continuum Mechanics and Material Theory, Computational Reality. http://www.lkm.tu-berlin.de/ComputationalReality/. Accessed 11 Jan 2019
2. Abali BE (2017) Computational reality, solving nonlinear and coupled problems in continuum mechanics. Advanced structured materials, vol 55. Springer, Singapore
3. Abali BE, Müller WH (2015) Numerical modeling of thermoelectric coupling. In: Elgeti S, Simon J-W (eds) Conference proceedings of the YIC GACM 2015, 3rd ECCOMAS young investigators conference, pp 1–4. Publication server of RWTH Aachen University
4. Abali BE, Queiruga AF (2019) Theory and computation of electromagnetic fields and thermomechanical structure interaction for systems undergoing large deformations. J Comput Phys 394:200–231
5. Abali BE, Reich FA (2017) Thermodynamically consistent derivation and computation of electro-thermo-mechanical systems for solid bodies. Comput Methods Appl Mech Eng 319:567–595
6. Abali BE, Reich FA (2018) Verification of deforming polarized structure computation by using a closed-form solution. Contin Mech Thermodyn. https://doi.org/10.1007/s00161-018-0709-8
7. Abali BE, Zohdi TI (2018) On the accuracy of reduced-order integrated circuit simulators for computing the heat production on electronic components. J Comput Electron 17(2):625–636
8. Alnaes MS, Mardal K-A (2010) On the efficiency of symbolic computations combined with code generation for finite element methods. ACM Trans Math Softw 37(1):6
9. Altenbach H, Altenbach J, Kissing W (2018) Mechanics of composite structural elements. Springer, Berlin
10. Bossavit A (1988) Whitney forms: a class of finite elements for three-dimensional computations in electromagnetism. IEE Proc A Phys Sci Meas Instrum Manag Educ Rev 135(8):493–500
11. Cheng L, Hannaford B (2015) Finite element analysis for evaluating liver tissue damage due to mechanical compression. J Biomech 48(6):948–955
12. Ciarlet P Jr, Zou J (1999) Fully discrete finite element approaches for time-dependent Maxwell's equations. Numer Math 82(2):193–219
13. Cooper MA (1995) Emergent care of lightning and electrical injuries. Semin Neurol 15:268–278
14. Cushing TA, Wright RK (2009) Electrical injuries. Emergency medicine web site. Available at: http://emedicine.medscape.com/article/770179-overview
15. Demkowicz L (2006) Computing with HP-adaptive finite elements: one and two dimensional elliptic and Maxwell problems, vol 1. CRC Press, Boca Raton
16. Eswaran SK, Bayraktar HH, Adams MF, Gupta A, Hoffmann PF, Lee DC, Papadopoulos P, Keaveny TM (2007) The micromechanics of cortical shell removal in the human vertebral body. Comput Methods Appl Mech Eng 196(31–32):3025–3032
17. Fontanarosa PB (1993) Electrical shock and lightning strike. Ann Emerg Med 22(2):378–387
18. Freitas RA (1999) Nanomedicine, volume I: basic capabilities, vol 1. Landes Bioscience, Georgetown
19. Fung YC (1967) Elasticity of soft tissues in simple elongation. Am J Physiol Leg Content 213(6):1532–1544
20. Fung YC (1983) On the foundations of biomechanics. J Appl Mech 50(4b):1003–1009
21. Gatewood MOK, Zane RD (2004) Lightning injuries. Emerg Med Clin 22(2):369–403
22. Gillette A, Rand A, Bajaj C (2016) Construction of scalar and vector finite element families on polygonal and polyhedral meshes. Comput Methods Appl Math 16(4):667–683
23. Giorgio I, Andreaus U, Lekszycki T, Corte AD (2017) The influence of different geometries of matrix/scaffold on the remodeling process of a bone and bioresorbable material mixture with voids. Math Mech Solids 22(5):969–987
24. GNU Public (2007) Gnu general public license. http://www.gnu.org/copyleft/gpl.html. Accessed 11 Jan 2019
25. Henriques FC Jr, Moritz AR (1947) Studies of thermal injury: I. The conduction of heat to and through skin and the temperatures attained therein. A theoretical and an experimental investigation. Am J Pathol 23(4):530
26. Holzapfel GA, Ogden RW (2009) Biomechanical modelling at the molecular, cellular and tissue levels, vol 508. Springer, Berlin
27. Humphrey JD (2013) Cardiovascular solid mechanics: cells, tissues, and organs. Springer, Berlin
28. Hutter K (1975) On thermodynamics and thermostatics of viscous thermoelastic solids in the electromagnetic fields. A Lagrangian formulation. Arch Ration Mech Anal 58(4):339–368
29. Kachanov L (1986) Introduction to continuum damage mechanics, vol 10. Springer, Berlin
30. Lance A (2018) https://grabcad.com/library/hand-export-from-3dmax-to-solidworks-1. Accessed 11 Jan 2019

31. Lederer W, Kroesen G (2005) Emergency treatment of injuries following lightning and electrical accidents. Der Anaesthesist 54(11):1120–1129
32. Li J (2009) Numerical convergence and physical fidelity analysis for Maxwell's equations in metamaterials. Comput Methods Appl Mech Eng 198(37):3161–3172
33. Logg A, Mardal KA, Wells GN (2011) Automated solution of differential equations by the finite element method, the FEniCS book. Lecture notes in computational science and engineering, vol 84. Springer, Berlin
34. Lorenz L (1867) On the identity of the vibrations of light with electrical currents. Lond Edinb Dublin Philos Mag J Sci 34(230):287–301
35. Moritz A, Moritz AR, Henriques FC Jr (1947) Studies of thermal injury: II. The relative importance of time and surface temperature in the causation of cutaneous burns. Am J Pathol 23(5):695
36. Nédélec J-C (1980) Mixed finite elements in R3. Numer Math 35(3):315–341
37. Niyonzima I, Jiao Y, Fish J (2019) Modeling and simulation of nonlinear electro-thermo-mechanical continua with application to shape memory polymeric medical devices. Comput Methods Appl Mech Eng 350:511–534
38. Oliphant TE (2007) Python for scientific computing. Comput Sci Eng 9(3):10–20
39. Pearce J (2018) Irreversible tissue thermal alterations: skin burns, thermal damage and cell death. Theory Appl Heat Transf Hum 2:553–590
40. Placidi L, Barchiesi E (2018) Energy approach to brittle fracture in strain-gradient modelling. Proc R Soc A Math Phys Eng Sci 474(2210):20170878
41. Queiruga AF, Zohdi TI (2016) Formulation and numerical analysis of a fully-coupled dynamically deforming electromagnetic wire. Comput Methods Appl Mech Eng 305:292–315
42. Raviart PA, Thomas JM (1977) A mixed finite element method for 2-nd order elliptic problems. In: Galligani I, Magenes E (eds) Mathematical aspects of finite element methods. Lecture notes in mathematics, vol 606. Springer, Berlin, Heidelberg, pp 292–315
43. Sapareto SA, Dewey WC (1984) Thermal dose determination in cancer therapy. Int J Radiat Oncol* Biol* Phys 10(6):787–800
44. Stephen A, Adams CA, Cioffi WG (2012) Electrical injury-high-voltage current. In: Vincent JL, Hall JB (eds) Encyclopedia of intensive care medicine. Springer, Berlin, Heidelberg, pp 820–822
45. Wright NT (2015) Quantitative models of thermal damage to cells and tissues. In: Heat transfer and fluid flow in biological processes, pp 59–76. Elsevier
46. Xu F, Lu TJ, Seffen KA (2008) Biothermomechanics of skin tissues. J Mech Phys Solids 56(5):1852–1884
47. Zohdi TI (2014) Modeling electrical power absorption and thermally-induced biological tissue damage. Biomech Model Mechanobiol 13(1):115–121
48. Zohdi TI, Abali BE (2018) Modeling of power transmission and stress grading for corona protection. Comput Mech 62(3):411–420
49. Zohdi TI (2018) Finite element primer for beginners. Springer, Berlin